JOURNAL OF MATERIALS SCIENCE 26 (1991) 4721–4726

Tensile force at break of gel-spun/hot-drawn ultrahigh molecular weight polyethylene fibres

J. P. PENNING, D. J. DIJKSTRA*, A. J. PENNINGS
Department of Polymer Chemistry, University of Groningen, Nijenborgh 16, 9747 AG Groningen, The Netherlands

Fibres obtained by gel spinning of ultrahigh molecular weight polyethylene (UHMWPE) were drawn to various ratios, and the improvement of the tensile strength of the hot-drawn filaments with increasing draw ratio has been studied. The tensile force at break of gel-spun/hot-drawn UHMWPE fibres appeared to be constant for draw ratios exceeding $\lambda = 30$. From scaling arguments, full chain extension is expected at this draw ratio. On the basis of development of the physical properties during drawing, it is concluded that little disentangling occurs up to $\lambda = 30$. Beyond this point, slippage of chains through entanglement hooks becomes predominant. The observed constant tensile force at break can be explained by this drawing mechanism.

1. Introduction

The preparation of polymeric fibres with high elastic moduli and tensile strengths has attracted much attention in the past decades. Polyethylene fibres and films, displaying excellent material properties, have been prepared by various routes, e.g. drawing of single-crystal mats [1], zone annealing [2], hydrostatic extrusion [3], as well as the technique of gel spinning and subsequent hot drawing [4, 5], the latter giving fibres with tensile strengths up to 7 GPa [6]. In these processes, a number of physical properties of the samples change dramatically with increasing extension or draw ratio.

In this paper, our attention will be mainly directed to the increase in strength that is observed for gel-spun/hot-drawn fibres, prepared from ultrahigh molecular weight polyethylene (UHMWPE). The strength of a fibre is calculated from the force at which the fibre breaks in the tensile test, divided by the cross-sectional area of this particular fibre. For draw ratios ranging from $\lambda = 30$ to 60, this tensile force appeared to be constant. Since the tensile force at break may be related to the absolute number of load-carrying chains in the fibre cross-section, the strength increase in this range of draw ratios seems to arise from a progressively more efficient packing of the same number of load-carrying chains in the fibre cross-section. At higher draw ratios, achieved by applying a two-step drawing process, a similar behaviour was observed. At attempt is made to explain this behaviour in terms of molecular events taking place during hot drawing. Since entanglements play an important role in extending the chains during drawing, their behaviour will be discussed in more detail on the basis of physical properties of the drawn fibres.

2. Experimental procedure

The linear polyethylene sample used in this study was Hifax 1900 (by Hercules) with $M_w = 4 \times 10^6$ g mol^{-1} and $M_n = 2 \times 10^5$ g mol^{-1}. The polyethylene was dissolved in paraffin oil containing 0.5% anti-oxidant by weight (2,6-di(t-butyl)-p-cresol) at 135 °C through mechanical stirring, at a concentration of 5% by weight. The solution was homogenized for 48 h at 150 °C under a nitrogen atmosphere. Upon slow cooling of the solution, a gel formed that was fed to a piston cylinder apparatus and subsequently homogenized at 190 °C for 3 h. The solution was extruded at this temperature through a conical die (entrance angle 6°, exit diameter 1 mm) at a speed of 1 m min^{-1} and wound onto a winding drum, without stretching the spinline. The solvent was removed from the gel fibres by extraction with n-hexane for 48 h. The extracted fibres were dried at 50 °C *in vacuo* while keeping them at constant length.

The as-spun fibres were stretched in an electric oven at 148 °C between two rolls, located outside the oven. The draw ratio was determined from the ratio of wind-up and feed velocities of the fibre. Fibre feed velocities ranging from 1.3 to 13 mm min^{-1} were used. The oven was gently flushed with nitrogen, in order to prevent oxidative degradation.

Mechanical properties of the fibres were determined using an Instron 4301 tensile testing machine, operating at a crosshead speed of 12 mm min^{-1}, using a sample gauge length of 32 mm. Cross-sectional areas were determined from the weight and length of the fibre, assuming a density of 1000 kg m^{-3}. Thermal properties were determined by differential scanning calorimetry (DSC), using a Perkin–Elmer DSC-7 operating at a scan speed of 10 °C min^{-1}. The crystallinity was determined from the ratio of the heat of fusion of the sample to the heat of fusion of perfectly crystalline polyethylene, which was taken 292.8 J g^{-1} [7]. Scanning electron microscopy (SEM) was performed on gold covered samples, using an ISI-DS 130 microscope operating at 40 kV.

Present address: Bayer AG, Corporate Research ZF-TPEI, Leverkusen, FRG.

0022–2461/91 $03.00 + .12

Shrinkage measurements were performed with constrained pre-heating [8]. A piece of ca. 50 cm was clamped between two stainless steel grips and heated to 150 °C, after which the distance between the grips was reduced until the fibre was lax. The shrinkage was determined from the reduction of distance between several ink marks on the fibre.

3. Results and discussion

A porous as-spun fibre of UHMWPE was drawn in a one-step drawing process to ratios of $\lambda = 10, 20, 25, 30, 35, 40, 50$ and 60, the latter being the maximum draw ratio that could be achieved by applying a one-step drawing process. Fibres having higher draw ratios were obtained by drawing a fibre with $\lambda = 30$ to the desired draw ratio. In this way, a maximum overall draw ratio of $\lambda = 100$ could be achieved.

Tensile tests were performed on fibres, obtained after drawing. From tensile tests, the strength of a fibre is calculated from the force at which the fibre breaks, as is recorded by the tensile tester, divided by the cross-sectional area of this particular fibre. In Fig. 1 the tensile force at break of hot-drawn fibres is presented as a function of draw ratio.

The tensile force at break of fibres, drawn in a one-step process, initially increases slightly with increasing draw ratio and reaches a constant value beyond $\lambda = 30$. Fibres obtained after a two-step drawing process (i.e. $\lambda \geq 70$) also show a tensile force at break that is independent of draw ratio, but its value is substantially lower than the tensile force at break of fibres prepared in a one-step process.

The tensile strength, calculated from tensile force at break data of hot-drawn fibres, is shown in Fig. 2 as a function of draw ratio. The maximum strength that can be achieved in a one-step drawing process is 3.8 GPa at a draw ratio of $\lambda = 60$. By applying a two-step process, the maximum attainable draw ratio is raised to $\lambda = 100$, giving a fibre with a tensile strength of 4 GPa. This demonstrates that the ultimate properties of the drawn fibre are not significantly improved by applying a two-step drawing process. Therefore it seems that the second drawing step merely changes the dimensions of the fibre, and no dramatic structural rearrangement, with respect to the mechanical properties of the fibre, takes place.

Fibres used for drawing experiments were obtained by extrusion of the spinning solution at a slow rate (1 m min^{-1}), without stretching the spinline. Under these conditions, the fibre obtained after extraction of the solvent consists of large lamellae that are connected by few fibrils. Upon hot drawing of the as-spun fibre, the lamellae are gradually transformed into smooth fibrils [5]. The basic structural element of this morphology is the microfibril, which can be visualized as a long array of extended-chain crystals, interrupted by disordered domains that originate from the presence of topological defects like chain entanglements [9]. Adjacent crystalline blocks are thought to be connected by taut tie molecules (TTM), traversing the disordered domains. These TTM may be segregated to form crystalline bridges that transmit the stress from one crystal block to the next upon sample loading [10]. The fraction of the disordered domains that is taken up by these load-carrying TTM, β, may be evaluated on the basis of a simplified morphological model of the microfibril structure described above [11]. In Fig. 3, the strength of the hot-drawn fibres used in this study is plotted as a function of the TTM

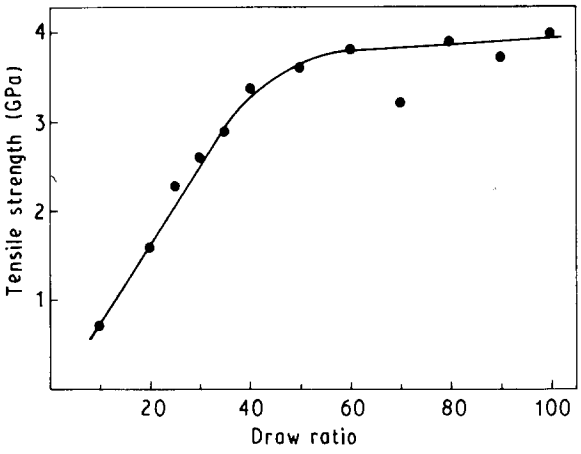

Figure 2 The tensile strength of gel-spun UHMWPE fibres, after hot drawing to various ratios.

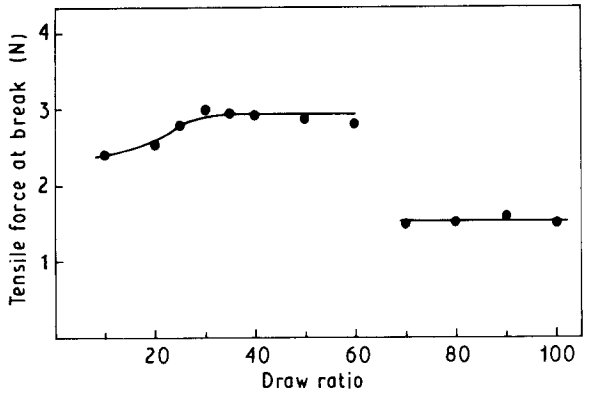

Figure 1 The tensile force at break of gel-spun/hot-drawn UHMWPE fibres as a function of draw ratio.

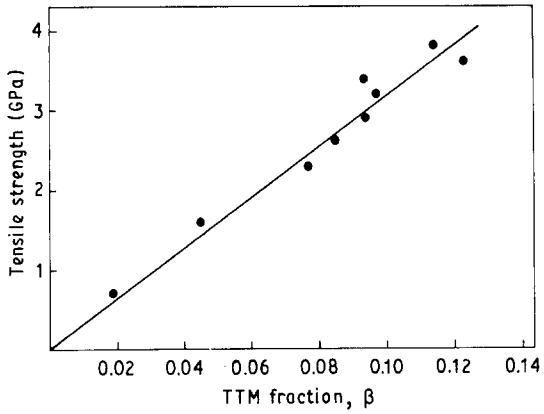

Figure 3 Relation between the strength of UHMWPE fibres with various draw ratios and the fraction of taut tie molecules (TTM) in the disordered domains.

fraction, calculated according to this model. Obviously, the strength of the fibre is closely related to the fraction of chains that transmit forces in the disordered domains. Furthermore, the stress concentration on the TTM, at the moment of sample failure, can be estimated from this relation by extrapolation to a TTM fraction of unity. In this way, a strength of 30 GPa is estimated for the tie molecules. This value coincides very well with the strength of the C–C bond derived from, for instance, Morse potential calculations [12, 13]. Sample failure, under the testing conditions applied, is therefore likely to be accomplished by rupturing the load-carrying tie molecules. The force required to break a sample can thus be related to the absolute number of chains ruptured in the fracture surface.

It is seen in Fig. 1 that the tensile force at break of hot-drawn fibres is practically constant for draw ratios ranging from $\lambda = 30$ to 60. This implies that the absolute number of load-carrying chains in the fibre cross-section, created in the drawing process, is about the same for a fibre with $\lambda = 30$ as it is for a fibre with $\lambda = 60$. Since the cross-sectional area of a drawn fibre progressively decreases with increasing draw ratio, this number of load-carrying chains is confined to a smaller cross-section in fibres with a higher draw ratio, which is expressed as an increasing tensile strength with increasing draw ratio (see Fig. 2). This observation may therefore yield valuable information on the processes at work during hot drawing, which are responsible for the improvement of mechanical properties upon drawing. A constant tensile force at break was also observed for dry-spun/hot-drawn poly(L-lactide) fibres and gel-spun/hot-drawn poly(vinyl alcohol) fibres [14].

In order to explain the observed tensile force at break behaviour, we will have to deal with the formation of tie molecules in the course of the drawing process. This is, however, an extremely complicated matter, since this process involves the deformation of a transient entanglement network and crystallization from the highly oriented melt, giving a fibre of a complex morphology. The formation of load-carrying chains will be closely related to the orientational changes that are induced by the elongational flow field in the drawing process. Chain entanglements play a very important role herein, in both polymer solution [15] and solids [16], and will be considered in more detail.

The concentration of entanglements in a polymer solution is generally expressed as the molecular weight of the chain section that connects two entanglements, M_e(sol). From scaling arguments, de Gennes [17] derived a relation between M_e(sol) and the volume fraction ϕ of polymer in the solution:

$$M_e(\text{sol}) = M_e(\text{melt})\,\phi^{-\alpha} \qquad (1)$$

where M_e(melt) represents the average molecular weight between entanglements in the polymer melt and α is a constant, determined by the quality of the solvent. De Gennes derived a value of $\alpha = 1.25$, when excluded volume effects are large, while Graessley and Edwards [18] report a value ranging from 1.0 to 1.3 for α. For solutions under θ-conditions, α can be calculated to be 2.0 [17]. Taking a value of 2000 kg kmol^{-1} for M_e(melt) [19], the average molecular weight between entanglements in the spinning solutions used in this study ($\phi = 0.05$) can be calculated to be 8.5×10^4 kg kmol^{-1} from this relation. This corresponds to a chain section comprising approximately 6.1×10^3 monomeric units.

From the average entanglement spacing calculated by this method, we can estimate the draw ratio at which the molecules become fully stretched between entanglements, referred to as the "maximum network draw ratio". This draw ratio, λ_n, corresponds to the ratio of the random coil dimensions ($2R_g$) to the contour length of the fully extended chain (L_c). In the case of polyethylene

$$\lambda_n = L_c/2R_g = 0.39\,n^{1/2} \qquad (2)$$

where n is the number of monomer units in the chain section of interest [8, 20]. From Equation 1, a value of $n = 6.1 \times 10^3$ was calculated for our system, which means that at a draw ratio of $\lambda = 30$ the molecules become fully extended between entanglements.

In the above calculation, it is tacitly assumed that no entanglements are lost in the course of the preparation process. In the spinning procedure, extrusion of the solution at a slow rate is followed by rapid crystallization (quenching to room temperature), which traps the entanglements between the crystallites formed. We therefore assume that the average entanglement spacing, calculated for the spinning solution, also holds for the as-spun fibre. During hot drawing, however, chain slippage through entanglement hooks is more likely to occur, due to the high drawing temperature and the low deformation rate. Since the maximum draw ratio that can be achieved in a one-step process exceeds $\lambda = 30$, this seems to be the case. This was also found by Smith *et al.* [21] for drawing of polyethylene films above 90 °C.

The question arises, at which stage of the drawing process these slippage events start to play an important role, since these processes will strongly affect the formation of tie molecules. Since the extension of the molecules between entanglements introduces orientation of the chains in the drawing direction, the development of orientation in the course of the drawing process may reveal the onset of slippage events. Information on the amount of molecular orientation and deformation efficiency can be obtained from, for instance, shrinkage data [22].

Shrinkage measurements were performed on gel-spun/hot-drawn UHMWPE fibres according to the "constrained pre-heating" method, in order to avoid "ribbon-shaped melting", which is usually observed when highly oriented samples are heated close to their melting point with free ends [8]. Fig. 4 shows an SEM micrograph of a fibre with $\lambda = 100$ that was shrunk by immersing it in silicone oil at 150 °C with free ends. Under these conditions, ribbon-shaped melting starts simultaneously at several weak spots on the fibre surface (e.g. kink bands). As a result of this, the shrinkage proceeds inhomogeneously and the fibre loses its original shape. In this way, unreliable shrinkage data

are obtained. When the fibre is shrunk according to the constrained preheating method, however, its cylindrical shape is maintained as shown in Fig. 5. Apparently, shrinkage of the fibre has taken place homogeneously and is not disturbed by melting effects. The nature of the longitudinal striations that can be observed on both samples is still unclear.

In Fig. 6, shrinkage data of gel-spun/hot-drawn UHMWPE fibres are presented as a function of draw ratio. As can be seen, the shrinkage displayed by hot-drawn filaments steeply increases with increasing draw ratio up to $\lambda = 30$, where this increase starts to deflect. This indicates an efficient orientation of the macromolecular chains (i.e. little disentangling) at draw ratios not exceeding $\lambda = 30$. At higher draw ratios, slippage of chains through the hooks formed by entanglements becomes predominant, as is reflected in a much slower increase of the shrinkage beyond $\lambda = 30$.

A similar trend can be observed in the crystallinity of drawn filaments as a function of draw ratio (Fig. 7). Initially, the lamellar structure of the as-spun fibre is partially destroyed, as is demonstrated by the decrease in crystallinity from 68 to 47% upon drawing the as-spun fibre to $\lambda = 10$. Drawing to higher ratios results in fibres with progressively higher crystallinities, up to $\lambda = 35$. In this range of draw ratios, the broad melting endotherm typical for the lamellar crystals in the starting material gradually shifts to higher temperatures and becomes much sharper. This results from the transformation from a lamellar to a fibrillar morphology, which is accomplished by an effective extension of the macromolecules between entanglements. At higher draw ratios, the melting point of the drawn fibre increases at a much slower rate with increasing draw ratio. Apparently, in this stage of the process, a more perfect crystal structure is achieved, but no dramatic morphological rearrangements take place.

These results are consistent with the observations of Anandakumaran *et al.* [23], who found that a number of physical properties (e.g. birefringence, crystallinity and melting point) of UHMWPE fibres reach a limiting value at the draw ratio at which full chain extension is expected. Our results indicate that slippage of chains through the hooks formed by entanglements begins near the point in the drawing process where the chains become fully extended between entanglements, i.e. near $\lambda = 30$, as was derived in a theoretical approach. Hadziioannou *et al.* [24] also found that, for coextrusion oriented polystyrene, the entanglements effectively hold to near the maximum network draw

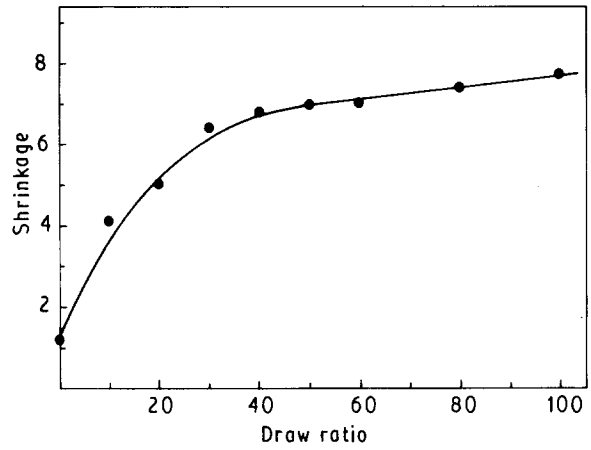

Figure 6 Shrinkage (the quotient of the sample length before and after constrained pre-heating shrinkage treatment) of gel-spun/hot-drawn UHMWPE fibres as a function of draw ratio.

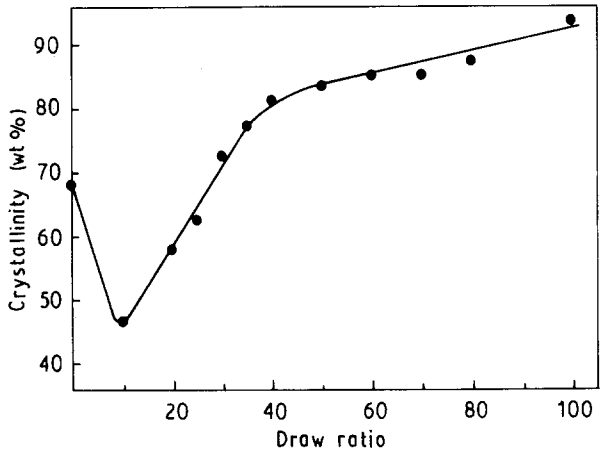

Figure 7 The crystallinity, calculated from heats of fusion, of hot-drawn filaments with various draw ratios.

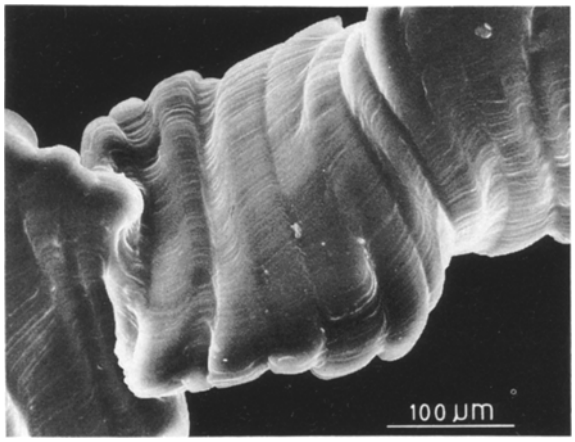

Figure 4 Scanning electron micrograph of a fibre wih $\lambda = 100$, after unconstrained shrinkage treatment.

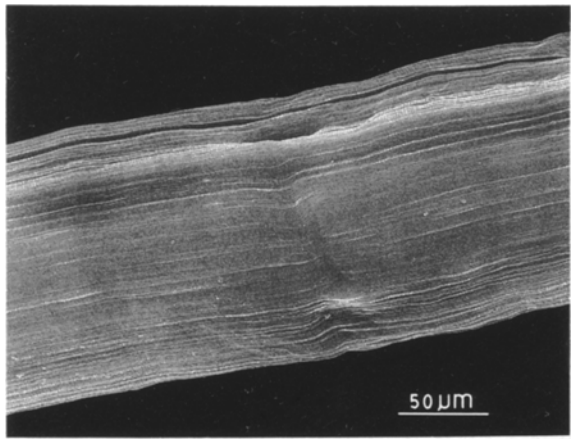

Figure 5 Scanning electron micrograph of a fibre with $\lambda = 100$, after shrinkage according to the constrained pre-heating method.

ratio, and that disentangling starts at higher ratios.

At low draw ratios, the lamellae in the as-spun fibre are transformed into fibrillar crystals upon drawing. This structural rearrangement is apparently accompanied by an increase of the tensile force at break of the drawn filament (see Fig. 1). This is not very surprising, however, since this process increases the number of chains that are aligned along the fibre axis. It was concluded that no substantial slip of chains through entanglement hooks occurs in this stage of the drawing process. Initially, only one-third of the network chains transmit forces in the fibre direction, as was pointed out by Bueche [25], and consequently only one-third of the network chains will be extended between the entanglement points. A similar behaviour is observed during cold drawing of UHMWPE [26]. During cold drawing, crazes are formed on the fibre surface, and these crazes are spanned by fibrils that are oriented in the draw direction. Initially the length of these fibrils increases with draw ratio, until a certain maximum fibril length is reached. Applying higher extensions results in the formation of more crazes. The maximum fibril length appeared to correspond very well to the contour length of molecular strands that are fully extended between entanglements.

In our hot-drawing experiments, slippage of chains through entanglement hooks becomes predominant when the maximum network draw ratio is exceeded. These slippage events allow elongation of the molecular strands oriented in the fibre direction, at the expense of the remaining material which is, in this way, pulled in the fibre direction through the entanglement hooks. This process reduces the fibre diameter and increases its length, while the number of chains that transmit forces in the fibre direction remains constant. This mechanism is consistent with the observation of a constant tensile force at break of drawn fibres in this particular range of draw ratios, since elongation of the fibre proceeds through slippage, rather than by breakage of load-carrying chains. This process will be accompanied by migration of entanglements that are acting as "slip-links" [27]. The maximum attainable draw ratio is likely to be limited by the accumulation of entanglements in complex topological defects and tight knots that cannot be removed upon drawing [28, 29].

By drawing in a second step, the maximum attainable draw ratio can be further enhanced to $\lambda = 100$. This increase, however, is not accompanied by a similar increase in strength. The tensile force at break of fibres, obtained after two-step drawing, is approximately two times lower than is displayed by the precursor with $\lambda = 30$. Apparently, load-carrying chains present in the fibre with $\lambda = 30$ are broken in the second drawing step. Considering the mechanical properties, it is clear that a much higher stress is required for the extension (at 148 °C) of a fibre with $\lambda = 30$ than it is for the extension of the as-spun fibre in the first drawing step. In other words, it will be more difficult to rearrange the mechanically coherent fibrillar crystals than to unfold the relatively weak lamellae. In the second drawing step, the stress required for drawing will cause fracture of a number of load-carrying chains, resulting in a lower tensile force at break of fibres obtained after the second draw. Since the second drawing step further reduces the fibre's cross-sectional area, the maximum strength that can be achieved in the two-step drawing process is about the same as the maximum strength that can be achieved in the one-step process.

4. Conclusions

In the drawing of gel-spun UHMWPE fibres, entanglements act as temporary physical cross-links and therefore they play an important role in the drawing process. The draw ratio at which the chains become fully extended between entanglements was estimated from scaling arguments and conformational statistics. Beyond this draw ratio, a number of physical properties of the drawn material improve less steeply with increasing draw ratio than is observed at lower draw ratios. These results suggest that little disentangling occurs up to the draw ratio at which full chain extension is expected. At higher draw ratios, slippage of chains through entanglement hooks becomes predominant. The constant tensile force at break observed in this range of draw ratios seems to be explained by these slippage events, since elongation of the fibre can take place without a decrease in the absolute number of chains that transmit forces in the fibre direction. When a fibre with a fibrillar morphology is subjected to hot drawing, the higher stress required for rearranging the extended chain crystals causes fracture of load-carrying chains. Consequently, drawing in a second step decreases the tensile force at break of the hot-drawn fibres. Therefore, the ultimate mechanical properties of the fibre are not significantly improved by hot-drawing in a second step.

Acknowledgements

The authors thank Dr A. R. Postema, Drs H. van der Werff and Ir M. Roukema for many helpful discussions. This study was financially supported by AKZO, The Netherlands.

References

1. T. KANAMOTO, A. TSURUTA, K. TANAKA, M. TAKEDA and R. S. PORTER, *Macromolecules* **21** (1988) 470.
2. T. KUNUGI, S. OOMORI and S. MIKAMI, *Polymer* **29** (1988) 614.
3. G. CAPACCIO, A. G. GIBSON and I. M. WARD, in "Ultra-high Modulus Polymers", edited by A. Ciferri and I. M. Ward (Applied Science, London, 1979) p. 20.
4. J. SMOOK, M. FLINTERMAN and A. J. PENNINGS, *Polym. Bull.* **2** (1980) 775.
5. A. J. PENNINGS and J. SMOOK, *J. Mater. Sci.* **19** (1984) 3443.
6. A. J. PENNINGS, D. J. DIJKSTRA, A. R. POSTEMA, M. ROUKEMA, W. HOOGSTEEN and H. van der WERFF, in "Frontiers of Macromolecular Science", edited by T. Saegusa, T. Higashimura and A. Abe (Blackwell Scientific, 1989) p. 357.
7. B. WUNDERLICH and G. CZORNYJ, *Macromolecules* **10** (1977) 906.
8. D. J. DIJKSTRA and A. J. PENNINGS, *Polym. Bull.* **19** (1988) 65.

9. J. SMOOK and A. J. PENNINGS, *Colloid Polym. Sci.* **262** (1984) 712.
10. A. PETERLIN, *Polym. Eng. Sci.* **19** (1979) 118.
11. J. P. PENING, H. van der WERFF, M. ROUKEMA and A. J. PENNINGS, *Polym. Bull.* **23** (1990) 347.
12. J. H. de BOER, *Trans. Faraday Soc.* **32** (1936) 10.
13. A. KELLY and N. H. MACMILLAN, in "Strong Solids", 3rd Edn (Oxford Science, Clarendon Press, Oxford, 1988) p. 7.
14. A. R. POSTEMA and B. J. LOMMERTS, personal communication.
15. A. CHOW, A. KELLER, A. J. MÜLLER and J. A. ODELL, *Macromolecules* **21** (1988) 250.
16. Y. TERMONIA and P. SMITH, *ibid.* **21** (1988) 2184.
17. P. G. de GENNES, in "Scaling Concepts in Polymer Physics" (Cornell University Press, Ithaca, New York, 1979) Ch. 3.
18. W. W. GRAESSLEY and S. F. EDWARDS, *Polymer* **22** (1981) 1329.
19. R. S. PORTER and J. F. JOHNSON, *Chem. Rev.* **66** (1966) 1.
20. P. A. IRVINE and P. SMITH, *Macromolecules* **19** (1986) 240.
21. P. SMITH, P. J. LEMSTRA and H. C. BOOIJ, *J. Polym. Sci., Polym. Phys. Edn* **19** (1981) 877.
22. M. P. C. WATTS, A. E. ZACHERIADES and R. S. PORTER, *J. Mater. Sci.* **15** (1980) 426.
23. K. ANADAKUMARAN, S. K. ROY and R. St. JOHN MANLEY, *Macromolecules* **21** (1988) 1746.
24. G. HADZIIOANOU, L. H. WANG, R. S. STEIN and R. S. PORTER, *ibid.* **15** (1982) 880.
25. F. BUECHE, in "Physical Properties of Polymers" (Interscience, New York, 1962) p. 237.
26. A. R. POSTEMA, W. HOOGSTEEN and A. J. PENNINGS, *Polym. Commun.* **28** (1988) 148.
27. R. C. BALL, M. DOI, S. F. EDWARDS and M. WARNER, *Polymer* **22** (1981) 1010.
28. P. G. de GENNES, *Macromolecules* **17** (1984) 703.
29. G. H. EDWARD and R. G. O'DONNELL, *J. Mater. Sci.* **21** (1986) 958.

Received 5 April
and accepted 10 October 1990